

Kinetics of the $C_6H_5 + O_2$ Reaction at Low Temperatures

T. Yu and M. C. Lin*

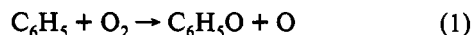
Contribution from the Department of Chemistry, Emory University, Atlanta, Georgia 30322

Received May 6, 1994*

Abstract: The kinetics of the $C_6H_5 + O_2$ reaction has been studied with the cavity-ring-down (CRD) method by monitoring the rate of $C_6H_5O_2$ radical formation at 496.4 nm. The second-order rate constants measured under the conditions, 20 Torr $\leq P \leq 80$ Torr (Ar), 297 K $\leq T \leq 473$ K, were found to be pressure-independent, with a small negative activation of 0.32 kcal/mol. A least-squares analysis of a dozen sets of data obtained by two different kinetic evaluation methods gives rise to $k_{O_2} = 10^{-11.00 \pm 0.08} \exp[(+161 \pm 66)/T]$ cm³/molecule-s where the errors represent one-standard deviations, evaluated with the weighting factors $w_i = (k_i/\sigma_i)^2$. Under the conditions employed in the present work, the $C_6H_5 + O_2$ reaction takes place primarily by the addition-stabilization process $C_6H_5 + O_2 \leftrightarrow C_6H_5O_2^{\ddagger} \xrightarrow{(+M)} C_6H_5O_2$. A search carried out at 575.4 nm for the production of C_6H_5O , which could be conveniently and sensitively detected by the CRD method, failed to detect the radical. This finding is fully consistent with the apparent large activation energy for the formation of C_6H_5O from the $C_6H_5 + O_2$ reaction (6 kcal/mol) recently reported by Frank and co-workers (ref 30) using the atomic resonance absorption-shock tube method at $T > 900$ K.

Introduction

The reaction of C_6H_5 with O_2 plays a pivotal role in the incipient soot formation process in hydrocarbon combustion reactions.^{1,2} At high temperatures, the reaction readily produces C_6H_5O which can undergo further fragmentation reaction,^{3,4} viz.,



and thus effectively retards the formation of polyaromatic hydrocarbons (PAHs), likely precursors of soot.^{1,5}

In a recent series of kinetic studies of C_6H_5 reactions in the gas phase, we have reported the results of the first successful attempt to measure their absolute rate constants relevant to soot formation,⁶⁻⁹ including the title reaction, $C_6H_5 + O_2$. In these studies, we employed a novel multipass laser absorption method using a high quality optical cavity, referred to as the cavity-ring-down (CRD) technique,⁶⁻¹¹ for the detection of the C_6H_5 radical at 504.8 nm. Kinetically reasonable rate constants have been obtained for its reactions with NO, C_2H_2 , C_2H_4 , $c-C_5H_{10}$, $c-C_6H_{12}$, HBr/DBr, CH_2O , among others. The result for the $C_6H_5 + NO$ reaction, $k_{NO} = 4.5 \times 10^{-12} \exp(+433/T)$ cm³/molecule-s, for example, compares reasonably well with those for other known radical association, $R + NO$, reactions.⁸ For the reactions of C_6H_5 with C_2H_2 ¹² and C_2H_4 ,¹³ the results of RRKM calculations indicated that our low-temperature (297–523 K) and high-pressure (20–60 Torr) data correlate well with those

measured by Stein and co-workers using a Knudsen cell flow reactor under low-pressure (1–10 mTorr) and high-temperature (1100–1300 K) conditions, assuming $k_{C_6H_5+C_6H_5} = 5 \times 10^{-12}$ cm³/molecule-s.^{14,15} The rate constants for the C_6H_5 reactions with $c-C_5H_{10}$ and $c-C_6H_{12}$ also compare favorably with the values determined in the liquid phase at low temperatures as well as in the gas phase at high temperatures.¹⁶ These findings render strong support for the CRD technique as a sensitive and reliable tool for kinetic measurements vis-à-vis the conventional multipass absorption method.¹⁷

The validity of the CRD technique for kinetic studies has also been confirmed by a measurement for the $NH_2 + NO$ reaction.^{8,18} The rate constants measured for the reaction in the temperature range of 297–673 K agree closely with the recommended values.¹⁹

For the $C_6H_5 + O_2$ reaction, however, our preliminary result measured at 297 K by monitoring the decay of C_6H_5 in the presence of excess amounts of O_2 , $k_{O_2} = 3.8 \times 10^{-15}$ cm³/molecule-s,⁶ was found to be inconsistent with those reported for the phenyl and substituted phenyl radical reactions occurring in the gas phase and the liquid phase.²⁰ For example, the rate constant for the C_6H_5 reaction evaluated on the basis of separate relative rate measurements at different temperatures in solution within the range 298–333 K, $k_{O_2} \sim (0.8-1.7) \times 10^{-11}$ cm³/molecule-s,²⁰ is some four orders of magnitude greater than our preliminary result obtained by monitoring the rate of C_6H_5 decay as mentioned above. This severe discrepancy, as will be resolved later, stems primarily from the contamination of coabsorption by the $C_6H_5O_2$ adduct at 504.8 nm which became severe at longer reaction times, and thus resulted in an apparent slower decay of the C_6H_5 radical.

In this study, we measured the rates of the $C_6H_5 + O_2$ reaction at temperatures between 297 and 500 K by monitoring the growth

* Abstract published in *Advance ACS Abstracts*, September 15, 1994.

- (1) Glassman, I. *Combustion*, 2nd ed.; Academic Press: New York, 1986.
- (2) Brezinsky, K. *Prog. Energ. Combust. Sci.* **1986**, *12*, 1.
- (3) Colussi, A. J.; Zabel, F.; Benson, S. W. *Int. J. Chem. Kinet.* **1977**, *9*, 161.
- (4) Lin, C. Y.; Lin, M. C. *J. Phys. Chem.* **1986**, *90*, 425.
- (5) Bittner, J. D.; Howard, J. B.; Palmer, H. B. *NATO Conference Series*, 6; *Materials Science*; Plenum Press: New York, 1983; Vol. 7, p 95.
- (6) Yu, T.; Lin, M. C. *J. Am. Chem. Soc.* **1993**, *115*, 4371.
- (7) Lin, M. C.; Yu, T. *Int. J. Chem. Kinet.* **1993**, *25*, 875.
- (8) Yu, T.; Lin, M. C. *J. Phys. Chem.* **1994**, *98*, 2105.
- (9) Yu, T.; Lin, M. C. *Int. J. Chem. Kinet.* **1994**, *26*, 771.
- (10) O'Keefe, A.; Deacon, D. A. G. *Rev. Sci. Instrum.* **1988**, *59*, 2544.
- (11) O'Keefe, A.; Scherer, J. J.; Cooksy, A. L.; Sheeks, R.; Heath, J.; Saykally, R. J. *Chem. Phys. Lett.* **1990**, *172*, 214.
- (12) Yu, T.; Lin, M. C.; Melius, C. F. Absolute Rate Constant for the Reaction of Phenyl Radical with Acetylene. *Int. J. Chem. Kinet.*, in press.
- (13) Yu, T.; Lin, M. C. Kinetics of the Phenyl Radical Reaction with Ethylene: An RRKM Theoretical Analysis of Low and High Temperature Data. *Combustion and Flame*, in press.

(14) Fahr, A.; Mallard, W. G.; Stein, S. E. *21st Symposium International on Combustion* [proceedings]; The Combustion Institute: Pittsburgh, PA, 1986; p 825.

(15) Fahr, A.; Stein, S. E. *22nd Symposium International on Combustion* [proceedings]; The Combustion Institute: Pittsburgh, PA, 1988; p 1023.

(16) Yu, T.; Lin, M. C., manuscript in preparation.

(17) Freidel, M.; Zellner, R. *Ber. Bunsenges. Phys. Chem.* **1989**, *93*, 1417.

(18) Diau, E. W.; Yu, T.; Wagner, M. A. G.; Lin, M. C. *J. Phys. Chem.* **1994**, *98*, 4034.

(19) Baulch, D. L.; Cobos, C. J.; Cox, R. A.; Esser, C.; Frank, P.; Just, Th.; Kerr, J. A.; Pilling, M. J.; Troe, J.; Walker, R. W.; Warnatz, J. *J. Phys. Chem. Ref. Data* **1992**, *21*, 411.

(20) Sommeling, P. M.; Mulder, P.; Louw, R.; Avila, D. V.; Luszyk, J.; Ingold, K. U. *J. Phys. Chem.* **1993**, *97*, 8361.

of the $\text{C}_6\text{H}_5\text{OO}$ peroxy radical at wavelengths where the C_6H_5 radical has no known absorption bands. These new data will be compared with relevant kinetic data obtained in the same temperature region. Additionally, the validity of the $\text{C}_6\text{H}_5\text{O}_2$ detection for k_{O_2} measurement and the effect of pressure observed experimentally will be interpreted in terms of the RRKM theory, similar to the calculation performed previously for the $\text{CH}_3 + \text{O}_2$ reaction.²¹

Experimental Section

A. Experimental Procedure and Data Acquisition. The cavity-ring-down (CRD) technique developed for the kinetic studies of the reactions of C_6H_5 and NH_2 radicals has been described in detail elsewhere.⁶⁻⁹ Briefly, a Pyrex flow tube sealed with a pair of highly reflective mirrors at both ends forms the resonant cavity. Two lasers were employed sequentially. The photodissociation laser (Lambda Physik LPX 105) was split into two beams and introduced into the reaction system to photolyze nitrosobenzene at 248 nm or acetophenone at 193 nm to produce the phenyl radicals. The two beams crossed at an angle of about 15° at the center of the flow reactor. The probing pulse from the second laser (Laser Photonics N_2 -laser-pumped dye laser) was injected into the system along the axis of the cavity through one of the two mirrors to detect the radicals by measuring the decay time of the dye laser pulse which had been lengthened from 8 ns to about 30 μs by the cavity in the absence of an absorbing species. The presence of absorbing species, such as C_6H_5 , shortens the photon decay time. The following relationship between the photon decay time, t_c , obtained in the presence of resonance absorption and t_c° in the absence of resonance absorption, has been derived⁶⁻⁹

$$1/t_c = 1/t_c^\circ + c\alpha/nL \quad (\text{I})$$

where c is the velocity of light, l is the length of the absorbing medium, α is the absorption coefficient, n is the index of refraction, and L is the length of the cavity (50 cm).

In our previous studies of phenyl kinetics, we measured the decay of the C_6H_5 radical by its absorption at 504.8 nm. Based on eq I, the concentration of C_6H_5 at t' after the photodissociation of $\text{C}_6\text{H}_5\text{NO}$ or $\text{C}_6\text{H}_5\text{COCH}_3$ is given by

$$1/t_c = 1/t_c^\circ + (c\epsilon/nL)[A]_0 e^{-k't'} \quad (\text{II})$$

in which the absorption coefficient α in eq I is replaced by $\epsilon[A]_t = \epsilon[A]_0 \exp(-k't')$, where $[A]_0$ is the initial C_6H_5 concentration and k' is the apparent first-order rate constant for its decay in the presence of an excess amount of a molecular reactant such as NO .

In the present case, because of the appearance of the unexpectedly broad and strong absorption by $\text{C}_6\text{H}_5\text{O}_2$ in the same spectral region (see Figure 1) at longer reaction times ($t' > 200 \mu\text{s}$), eq II failed to provide any meaningful determination of k' by phenyl decay measurements, as we had encountered in our preliminary investigation. On the other hand, if the $\text{C}_6\text{H}_5\text{O}_2$ adduct is stable under the conditions studied, its rise time can be used for determining the rate constant of the $\text{C}_6\text{H}_5 + \text{O}_2$ reaction; for this purpose, eq II can be transformed into the expression

$$1/t_c = 1/t_c^\circ + (c\epsilon/nL)[A]_0(1 - e^{-k't'}) \quad (\text{III})$$

The validity of this equation will be illustrated later.

At long reaction times ($t' \rightarrow \infty$) when all of the C_6H_5 radicals are converted to $\text{C}_6\text{H}_5\text{O}_2$, eq III becomes

$$1/t_c^\infty = 1/t_c^\circ + (c\epsilon/nL)[A]_0 \quad (\text{IV})$$

Combination of eqs III and IV followed by a straightforward rearrangement gives rise to

$$\ln[t_c/(t_c - t_c^\infty)] = B + k't' \quad (\text{V})$$

where $B = \ln[t_c^\circ/(t_c^\circ - t_c^\infty)]$, which is constant in each experimental run. According to eq V, a plot of $\ln[t_c/(t_c - t_c^\infty)]$ vs t' should yield a straight line, whose slope gives k' , the first-order rate constant for the formation

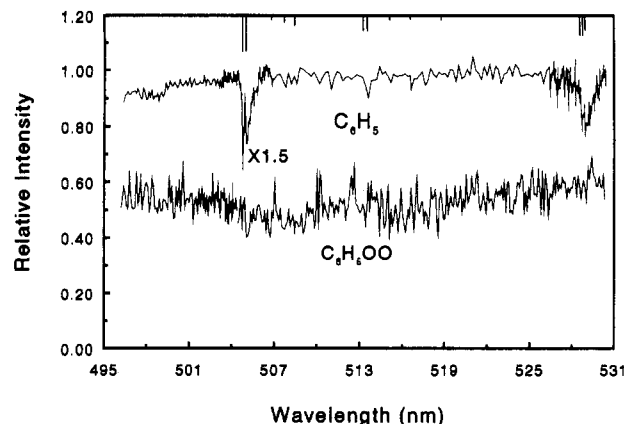


Figure 1. Absorption spectra of aromatic radicals in the visible range. Upper spectrum: phenyl radical. Both $\text{C}_6\text{H}_5\text{NO}$ and $\text{C}_6\text{H}_5\text{COCH}_3$ were used as radical sources. The vertical bars drawn on the wavelength axis show the positions and relative intensities of C_6H_5 absorption peaks by Porter and Ward.²² Lower spectrum: phenyl peroxy radical. A $\text{C}_6\text{H}_5\text{COCH}_3/\text{O}_2/\text{Ar}$ mixture was used to generate the radical at 193 nm with $[\text{O}_2] = 5 \times 10^{15} \text{ molecules/cm}^3$.

of $\text{C}_6\text{H}_5\text{O}_2$ under the condition that $[\text{C}_6\text{H}_5] \ll [\text{O}_2]$. Both eqs III and V will be utilized for the evaluation of k' in the presence of varying amounts of O_2 . A linear plot of the evaluated k' vs $[\text{O}_2]$ provides the second-order rate constant from its slope, k'' , for the association reaction $\text{C}_6\text{H}_5 + \text{O}_2 \rightarrow \text{C}_6\text{H}_5\text{O}_2$.

B. Chemicals. $\text{C}_6\text{H}_5\text{NO}$ (97%) and $\text{C}_6\text{H}_5\text{COCH}_3$ (99%) were obtained from Aldrich. They were used after extensive pumping and degassing. Anisole ($\text{C}_6\text{H}_5\text{OCH}_3$, 99%, Aldrich) was used as the source of $\text{C}_6\text{H}_5\text{O}$ for establishment of its detection by the CRD method. Both the molecular reactant, O_2 , and the carrier gas, Ar, acquired from Specialty Gases Southeast, were of UHP purity; they were used without further purification.

The concentration of O_2 was determined from measurement of its mass flow rate using a calibrated mass flowmeter (MKS). The total pressure of the reaction mixture was measured with an MKS Baratron manometer, which was directly connected to the reactor with a 9.5 mm o.d. flexible stainless steel tubing.

Results

A. Absorption Spectra of C_6H_5 , $\text{C}_6\text{H}_5\text{O}_2$, and $\text{C}_6\text{H}_5\text{O}$. Figure 1 presents the absorption spectra of C_6H_5 and $\text{C}_6\text{H}_5\text{O}_2$ obtained from separate scans. The spectrum of the phenyl radical was acquired from the photolysis of a small amount of $\text{C}_6\text{H}_5\text{NO}$ at 248 nm or $\text{C}_6\text{H}_5\text{COCH}_3$ at 193 nm in the absence of O_2 . The absorption peaks appeared in the vicinity of 505 nm have been published recently;^{6,8} the peak positions agree closely with those reported by Porter and Ward in 1965 using the flashphotolysis-spectrophotometry technique.²² The second absorption peak at 529 nm, measured by CRD for the first time, is also consistent with the one reported by Porter and Ward.

The strengths of these phenyl absorption bands are seen to be approximately one third that of the continuous absorption spectrum of the new species formed in the photolysis of $\text{C}_6\text{H}_5\text{NO}$ or $\text{C}_6\text{H}_5\text{COCH}_3$ in the presence of an excess amount of O_2 under the same conditions in which the phenyl absorption spectrum was taken in the absence of O_2 . The scan was carried out at $t' \geq 50 \mu\text{s}$ after photodissociation to allow for complete removal of the C_6H_5 radical by O_2 . Since no absorption by O_2 was detected in the absence of $\text{C}_6\text{H}_5\text{NO}$ or $\text{C}_6\text{H}_5\text{COCH}_3$ and the absorption spectrum obtained with either C_6H_5 source molecule was essentially identical, the new species responsible for the broad absorption is believed to be the phenylperoxy ($\text{C}_6\text{H}_5\text{O}_2$) radical, rather than the phenoxy ($\text{C}_6\text{H}_5\text{O}$) radical, whose absorption

(21) Hsu, D. S. Y.; Shaub, W. M.; Creamer, T.; Gutman, D.; Lin, M. C. *Ber. Bunsenges. Phys. Chem.* **1983**, *87*, 909.

(22) Porter, G.; Ward, B. *Proc. Roy. Soc. London* **1965**, *287*, 457.

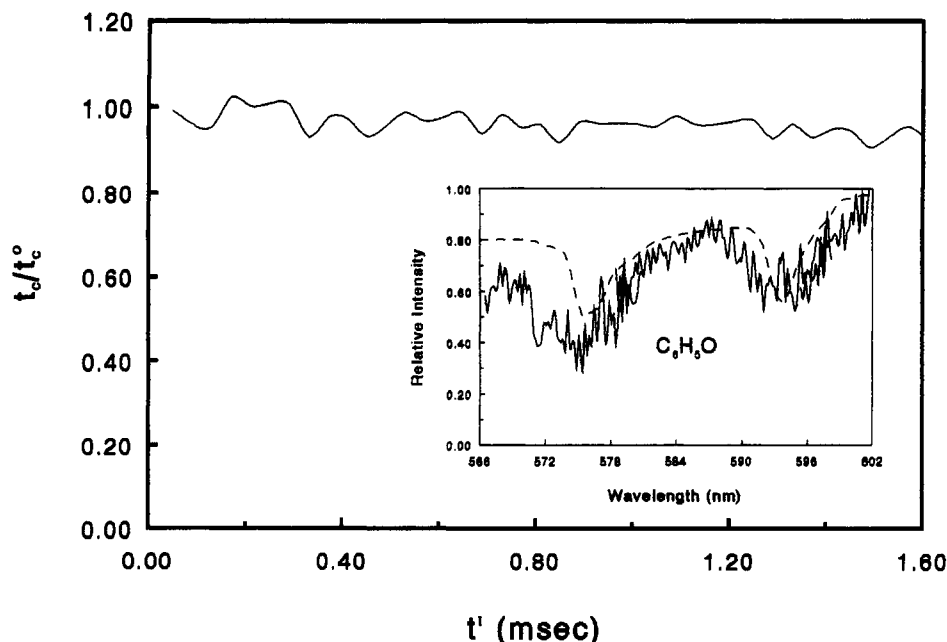


Figure 2. The relative cavity photon decay time profile measured after the photolysis of the $C_6H_5NO/O_2/Ar$ mixture by probing at $\lambda = 575.4$ nm. The system was irradiated by the KrF (248 nm) laser at 473 K. The lack of absorption indicates no C_6H_5O production. The inset is the absorption spectrum of C_6H_5O obtained by photolysis of $C_6H_5OCH_3$ at 193 nm. The dashed line in the inset shows the absorption spectrum of C_6H_5O obtained by Ward.²⁶

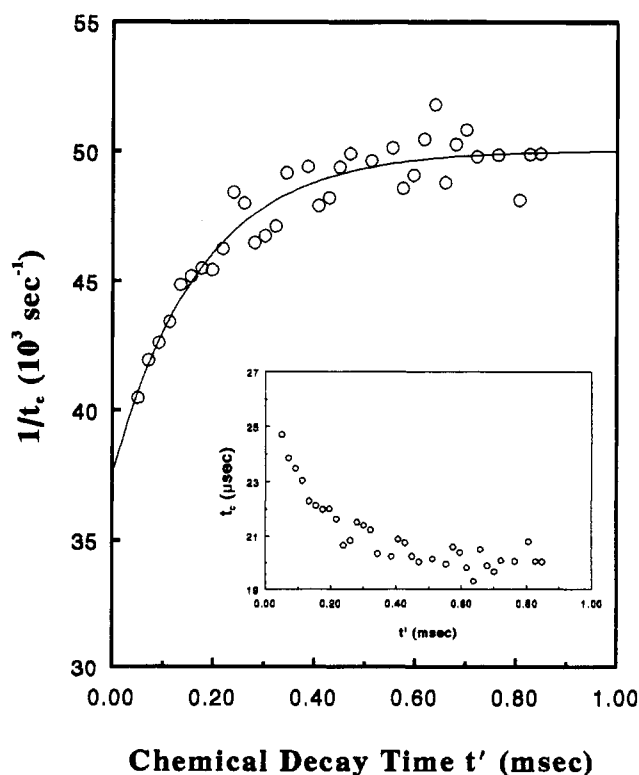


Figure 3. Typical inverse photon decay time plot obtained by the photolysis of $C_6H_5NO/O_2/Ar$ mixture at 248 nm. The measurement was carried out at 333 K with $[O_2] = 3.8 \times 10^{14}$ molecules/cm³. Probing laser was operated at 496.4 nm. The solid curve is the best fit to eq III.

spectra above 200 nm have been reported by Porter, Ward and others.^{23–26} Recently, similar absorptions near 500 nm in aqueous solutions have been reported for the phenylperoxy radical ($\lambda_{max} = 490$ nm)²⁷ as well as the 4-carboxyphenyl peroxy radical ($-O_2-CC_6H_4O_2$).²⁰

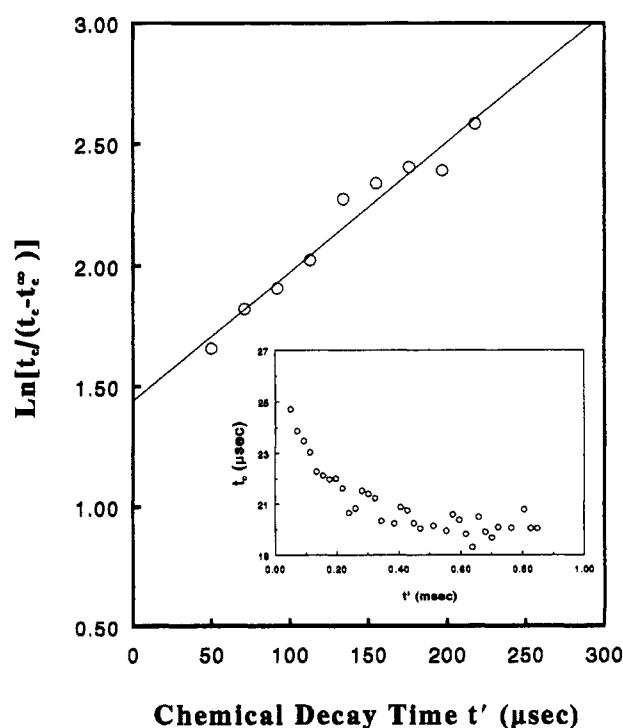


Figure 4. Representative plot for eq V. The experimental data used are the same as those presented in Figure 3.

To demonstrate that the C_6H_5O radical was not generated in the $C_6H_5 + O_2$ reaction within the temperature range studied, we have measured the appearance of C_6H_5O at 473 K, the highest temperature investigated, using its strongest absorption peak at 575 nm. No absorption by C_6H_5O was detected as illustrated in Figure 2. In the inset of the same figure, we have presented the first CRD absorption spectrum of C_6H_5O , produced by the photolysis of anisole at 193 nm; our spectrum agrees closely with that reported by Ward who employed the flash photolysis-spectrophotometry method.²⁶ This result indicates that the $C_6H_5 + O_2$ reaction does not produce $C_6H_5O + O$ at low temperatures despite its exothermicity ($\Delta H = -7$ kcal/mol), fully consistent with the result of our RRKM calculation to be presented later.

(23) Porter, G.; Ward, B. J. *Chim. Phys.* **1964**, *61*, 1517.

(24) Porter, G.; Wright, F. J. *Trans. Faraday Soc.* **1955**, *51*, 1469.

(25) Land, E. J.; Porter, G.; Strachan, E. *Trans. Faraday Soc.* **1961**, *57*, 1885.

(26) Ward, B. *Spectrochim. Acta*, **1968**, *24A*, 813.

(27) Mertens, R., von Sonntag, C., private communication.

Table 1. Evaluated First-Order and Second-Order Rate Constants for the Formation of C₆H₅O₂ at 398 K, Using Two Different Methods

$k'(\text{s}^{-1})$		$[\text{O}_2] (10^{14} \text{ molecules/cm}^3)$
eq III	eq V	
1621	1954	0.618
1992	1803	0.643
2416	2559	1.23
2859	3168	1.28
3078	2977	1.42
4660	3747	2.38
4681	4307	2.39
5037	5087	2.71
4930	4891	2.77
5146	5919	3.11
5704	5704	3.60
5356	5938	3.85
6945	6680	4.44
6915	7196	4.57

$$k'' = (1.27 \pm 0.07) \times 10^{-11} \quad k'' = (1.30 \pm 0.07) \times 10^{-11}$$

B. Kinetic Data Analysis. The rate constant for the appearance of the new absorbing species, C₆H₅O₂, from the photolysis of C₆H₅NO or C₆H₅COCH₃ in the presence of varying amounts of O₂, was analyzed by the two different methods described in the Experimental Section. With the first method based on eq III, which can be parameterized as

$$1/t_c = a + b(1 - e^{-ct'}) \quad (\text{VI})$$

with $a = 1/t_c^\infty$, $b = (cle/nL)[A]_0$, and $c = k'$, an entire time-resolved C₆H₅O₂ formation profile can be fitted by least-squares to obtain the first-order rate coefficient k' , as illustrated in Figure 3 for the reaction at 333 K.

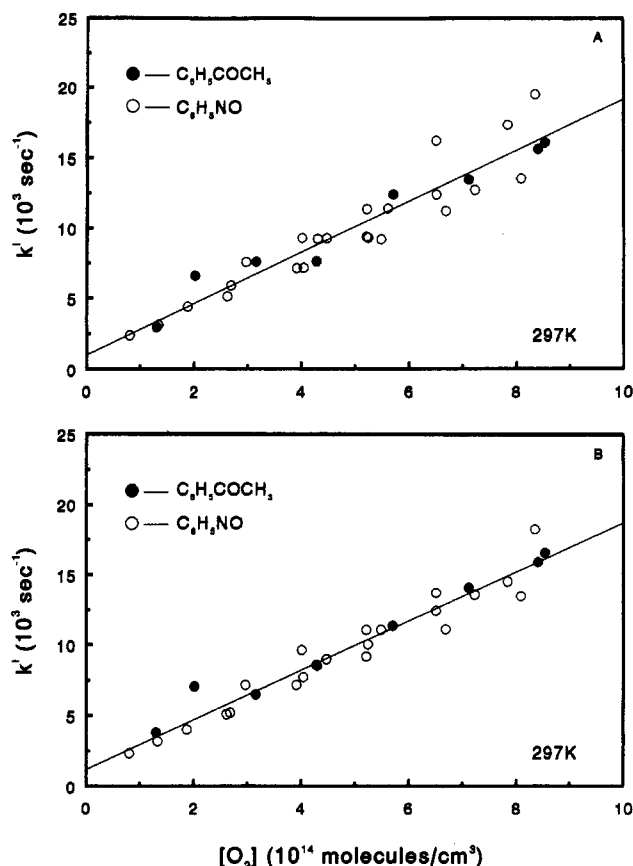
With the second method using eq V, only the data points obtained in the plateau t_c^∞ and the portion of the profile with $(t_c)^{-1}/(t_c^\infty)^{-1} \leq 0.9$ were utilized for k' evaluation. Figure 4 illustrates the existence of the linear relationship between $\ln[t_c/(t_c - t_c^\infty)]$ and t' , the chemical reaction time as predicted by eq V.

Table 1 compares the results of the analyses by these methods for the complete set of data acquired at 398 K with varying amounts of O₂. The second-order rate constants, obtained from the plots of k' vs $[\text{O}_2]$ as illustrated in Figure 5 using the data evaluated by eqs III and V, $k'' = (1.27 \pm 0.07) \times 10^{-11}$ and $(1.30 \pm 0.07) \times 10^{-11} \text{ cm}^3/\text{molecule}\cdot\text{s}$, respectively, agree with each other within the errors estimated by the least-squares method. Table 2 summarizes all results obtained in this study for the temperature range 297–473 K using the two methods of analysis. At 423 K, we have also investigated the effect of pressure by quadrupling it from 20 to 80 Torr; no noticeable effect was observed on the basis of the results of the two analyses. The averages of the two sets of k'' are presented graphically in Figure 6A in comparison with the temperature dependence of C₆H₅O₂ formation predicted by the RRKM theory for 1, 40, and 760 Torr pressures. The calculation was made with the formulation previously derived for the analogous CH₃ + O₂ reaction, which also has three product channels including the stabilization process.²¹ As indicated in Table 2, most of our experiments were performed at the constant pressure of 40 Torr using Ar as the diluent. These results are effectively in the high-pressure limit. A least-squares analysis of all the data presented in Table 2 gives

$$k_{\text{O}_2} = 10^{-11.00 \pm 0.08} \exp[(161 \pm 66)/T] \text{ cm}^3/\text{molecule}\cdot\text{s}$$

where the errors represent one-standard deviations, evaluated by using the weighting factor $w_i = (k_i/\sigma_i)^{2.28}$. Comparison of our result with other low-temperature data measured in the gas phase and in solution will be made later.

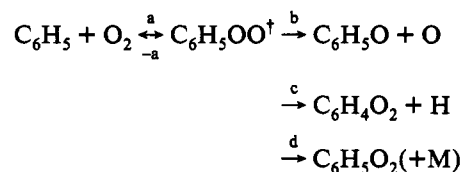
(28) Cvetanovic, R. J.; Singleton, D. L.; Paraskevopoulos, G. *J. Phys. Chem.* 1979, 83, 50.

**Figure 5.** Plots of k' vs $[\text{O}_2]$ at 297 K: (A) k' evaluated by eq III and (B) k' evaluated by eq V. Both C₆H₅NO (photolyzed at 248 nm, open circles) and C₆H₅COCH₃ (photolyzed at 193 nm, filled circles) were used as the source of the C₆H₅ radical. Linear least-squares fits to these plots yield the second-order rate constants, k'' , from their slopes.**Table 2.** Measured Bimolecular Rate Constants for C₆H₅ + O₂ at Different Temperatures

T (K)	P^a (Torr)	$[\text{O}_2]^b (10^{14}/\text{cm}^3)$	$k''^b (10^{-11} \text{ cm}^3 \cdot \text{s}^{-1})$	
			eq III	eq V
297 ^c	40	0–8.5	1.81 ± 0.11	1.75 ± 0.08
313	40	0–6.0	1.64 ± 0.09	1.82 ± 0.12
333	40	0–6.0	1.53 ± 0.08	1.43 ± 0.10
353	40	0–5.5	1.63 ± 0.16	1.71 ± 0.15
373	40	0–5.0	1.84 ± 0.17	1.90 ± 0.14
398	40	0–4.6	1.27 ± 0.07	1.30 ± 0.07
423	20	0–2.7	1.27 ± 0.20	1.66 ± 0.21
	40	0–4.1	1.49 ± 0.15	1.43 ± 0.17
	80	0–5.2	1.43 ± 0.08	1.55 ± 0.07
448	40	0–3.3	1.58 ± 0.11	1.73 ± 0.17
473	40	0–3.6	1.46 ± 0.18	1.53 ± 0.15

^a Mostly Ar. ^b cm³ and cm³/molecule·s are the common abbreviations for molecules/cm³ and cm³/molecule·s, respectively; errors represent 1σ's. ^c C₆H₅NO and C₆H₅COCH₃ were used as the C₆H₅ radical source by photolyzing at 248 and 193 nm, respectively. The former was employed exclusively for other temperatures on account of the convenience in operating the photodissociation laser at 248 nm.

In Figure 6B we compare the calculated rate constants for the three possible product channels



The calculation was performed on the basis of the Arrhenius parameters for channels (b) and (c) recently reported by Frank

and co-workers^{29,30} above 900 K using a shock tube under highly diluted conditions: $k_b = 4.3 \times 10^{-11} \exp(-3080/T)$ and $k_c = 5.0 \times 10^{-11} \exp(-4520/T) \text{ cm}^3/\text{molecule}\cdot\text{s}$. The kinetics and mechanism of this reaction will be further discussed in the following section.

Discussion

The photolysis of either C_6H_5NO at 248 nm or $C_6H_5COCH_3$ at 193 nm in the presence of an excess amount of O_2 was found to produce a new species, which absorbs broadly and strongly between 495 and 531 nm. Since both O_2 and the aromatic source molecules are required for the appearance of the broad absorption and the C_6H_5O radical was shown to be absent at the highest temperature (473 K) studied, the new species is concluded to be the phenylperoxy, $C_6H_5O_2$, radical.

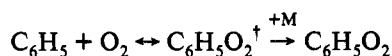
The evaluated Arrhenius parameters, $k_{O_2} = 10^{-11.0} e^{+161/T} \text{ cm}^3/\text{molecule}\cdot\text{s}$, with a negative activation energy of 0.32 kcal/mol, support the radical-molecular addition-stabilization process for the $C_6H_5O_2$ formation. These parameters, interestingly, give much higher values of rate constant than those of the analogous process, $CH_3 + O_2 \rightarrow CH_3O_2$, recently recommended for the high-pressure limit

$$k_{CH_3+O_2} = 1.3 \times 10^{-15} T^{1.2} \text{ cm}^3/\text{molecule}\cdot\text{s}^{19}$$

The equation gives $1.2 \times 10^{-12} \text{ cm}^3/\text{molecule}\cdot\text{s}$ at 297 K and $2.1 \times 10^{-12} \text{ cm}^3/\text{molecule}\cdot\text{s}$ at 473 K. Accordingly, toward O_2 , C_6H_5 is about 10 times more reactive than CH_3 .

Our low-temperature Arrhenius parameters differ significantly from those reported recently by Frank and co-workers^{29,30} based on the production of O and H atoms from the $C_6H_5 + O_2$ reaction above 900 K as referred to in the preceding section. Their large apparent activation energies of 6.1 and 9.0 kcal/mol for channels (b) and (c), respectively, rule out the significance of these bimolecular processes under the conditions employed in the present study.

The result of our preliminary multichannel RRKM calculation shown in Figure 6 also firmly supports the conclusion that under our experimental conditions ($T \leq 473 \text{ K}$, $P = 20\text{--}80 \text{ Torr}$), the $C_6H_5 + O_2$ reaction is dominated by the addition-stabilization process via channel (d)



The energetics and molecular parameters used in the calculation are summarized in the Appendix; they are based on our ab initio molecular orbital data for the $C_6H_5O_2$ radical and the rate constants for the $C_6H_5 + O_2$ addition obtained in this study and those for the production of $C_6H_5O + O$ and $C_6H_4O_2 + H$ by Frank et al.³⁰ Our detection of the $C_6H_5O_2$ radical below 473 K is fully consistent with the calculated strong dissociation energy, $D(C_6H_5 - O_2) = 41 \text{ kcal/mol}$, which agrees reasonably well with the value (37 kcal/mol) estimated by the correlation between $D(C_6H_5 - X)$ and $D(CH_3 - X)$, where X represents the substituent atoms or groups.³² The theoretical calculations and mechanism of this important reaction system will be discussed in greater detail later when more accurate pictures of the transition states involved in the reaction emerge from our extensive MO calculations which are underway. The molecular parameters (structures and vibrational frequencies) and the heats of formation of various stable $C_6H_5O_2$ isomers are presented in a companion article.³¹

Table 3. Molecular and Approximate Transition-State Parameters Used in the RRKM Calculation

species of transition state	$\Delta H_{f,0}^\circ$ (kcal/mol)	i	I_i ($10^{-40} \text{ g}\cdot\text{cm}^2$)	ν_j 's (cm^{-1})
$C_6H_5^a$	83	A	135.3	361, 389, 569, 572,
		B	150.8	613, 675, 759, 822,
		C	286.7	884, 894, 920, 947, 972, 999, 1101, 1110, 1244, 1251, 1392, 1413, 1464, 1487, 2994, 3002, 3012, 3018, 3023
O_2	0	A	0.0	1580
		B	77.5	
		C	77.5	
$C_6H_5O_2^*(a)^b$	83	A	150.0	90, 374(2), 600(4)
		B	670.1	880(8), 1170(4),
		C	900.	1450(5), 3029(5)
$C_6H_5O_2^a$	43	3lr	32.	
		A	160.0	227, 261, 409, 433,
		B	515.1	493, 598, 602, 680,
		C	675.2	758, 788, 842, 918,
$C_6H_5O_2^*(b)^c$	75.5	Ir	16.6	974, 981, 1000, 1004, 1053, 1090, 1128, 1148, 1192, 1220, 1315, 1453, 1488, 1609, 1611, 3004, 3014, 3026, 3035, 3064
		A	140.0	100(3), 200(2), 400(3),
		B	650.0	600(5), 950(8),
		C	900.0	1360(6), 3020(5)
$C_6H_5O_2^*(c)^c$	12.5	A	160.0	100(3), 400(6), 700(6),
		B	510.0	900(2), 1000(6),
		C	670.0	1300(5), 3020(4)

^a Molecular parameters obtained from ref 31. ^b Transition-state parameters obtained by fitting the rate constant for $C_6H_5O_2$ formation measured in the present study. ^c Transition-state parameters obtained by fitting k_b and k_c for the production of O and H, respectively, by Frank and co-workers (ref 30).

Comparison with Other Low-Temperature Kinetic Data. Reaction in the Gas Phase. Baldwin et al.³³ studied the oxidation of C_6H_6 in slowly reacting mixtures of H_2 and O_2 at 773 K and 500 Torr pressure using N_2 as diluent. On the basis of the measured benzene and total pressure changes, they obtained a "preliminary value" for the overall rate constant of the $C_6H_5 + O_2$ reaction, $k_{O_2} = 5.3 \times 10^{-13} \text{ cm}^3/\text{molecule}\cdot\text{s}$. This result is substantially lower than ours as illustrated in Figure 6A. Preidel and Zellner¹⁷ attempted to measure k_{O_2} with a multipass absorption method using a cw Ar^+ ion laser operating at 488 nm but failed to detect the reaction. They set an upper limit of $2 \times 10^{-17} \text{ cm}^3/\text{molecule}\cdot\text{s}$ for k_{O_2} (see Figure 6A). Since $C_6H_5O_2$ absorbs strongly in this spectral region as discussed before, the slow decay of the absorption measured in their experiment must correspond to the disappearance of the $C_6H_5O_2$ adduct.

From a kinetic study on the chlorination of C_6H_5Cl in the presence of O_2 at 603 K, Louw and co-workers^{20,34} concluded that the rate constant for $C_6H_4Cl + O_2 \rightarrow C_6H_4ClO_2$ should be at least as large as $1.7 \times 10^{-13} \text{ cm}^3/\text{molecule}\cdot\text{s}$. This conclusion is consistent with our data.

Reaction in Solution. In 1963, Russell and Bridger^{35,36} studied the reactivity of C_6H_5 toward O_2 in CCl_4 , $c\text{-}C_6H_{12}$, and mixed $CCl_4/c\text{-}C_6H_{12}$ solutions at 333 K. They obtained the relative rate constants $k_{O_2}/k_{CCl_4} = 630\text{--}1300$ and $k_{O_2}/k_{C_6H_{12}} = 640\text{--}1400$,³⁶ implying that $k_{C_6H_{12}}/k_{CCl_4} = 1.0$ as measured in a separate study without O_2 .³⁵ Combining the former with the absolute rate constant obtained at 318 K by Lorand and co-workers,³⁷ $k_{CCl_4} = (4.5\text{--}9.6) \times 10^{-15} \text{ cm}^3/\text{molecule}\cdot\text{s}$ (which compares well with the value reported by Scaiano and Stewart³⁸ at 298 K, $k_{CCl_4} = 1.3 \times 10^{-14} \text{ cm}^3/\text{molecule}\cdot\text{s}$), we have $k_{O_2} = (0.3\text{--}1.1) \times 10^{-11} \text{ cm}^3/\text{molecule}\cdot\text{s}$. A similar calculation with the $k_{O_2}/k_{C_6H_{12}}$ ratio given

(29) Herzler, J.; Frank, P. *Third International Conference on Chemical Kinetics*; NIST, Gaithersburg, MD, July 12–16, 1993.

(30) Frank, P.; Herzler, J.; Just, Th.; Wahl, C. *25th Symposium (International) on Combustion*, submitted for publication.

(31) Mebel, A. M.; Lin, M. C. *J. Am. Chem. Soc.*, submitted for publication.

(32) Lin, C.-Y. Ph.D. Dissertation, The Catholic University of America, Washington, DC, 1986.

(33) Baldwin, R. R.; Scott, M.; Walker, R. W. *21st Symposium (International) on Combustion*; The Combustion Institute, 1986; p 991.

(34) Dorrepaal, W.; Louw, R. *Int. J. Chem. Kinet.* **1978**, *10*, 249.

(35) Bridger, R. F.; Russell, G. A. *J. Am. Chem. Soc.* **1963**, *85*, 3754.

(36) Russell, G. A.; Bridger, R. F. *J. Am. Chem. Soc.* **1963**, *85*, 3765.

(37) Kryger, R. G.; Lorand, J. P.; Stevens, N. R.; Herron, N. R. *J. Am. Chem. Soc.* **1977**, *99*, 7589.

(38) Scaiano, J. C.; Stewart, L. C. *J. Am. Chem. Soc.* **1983**, *105*, 3609.

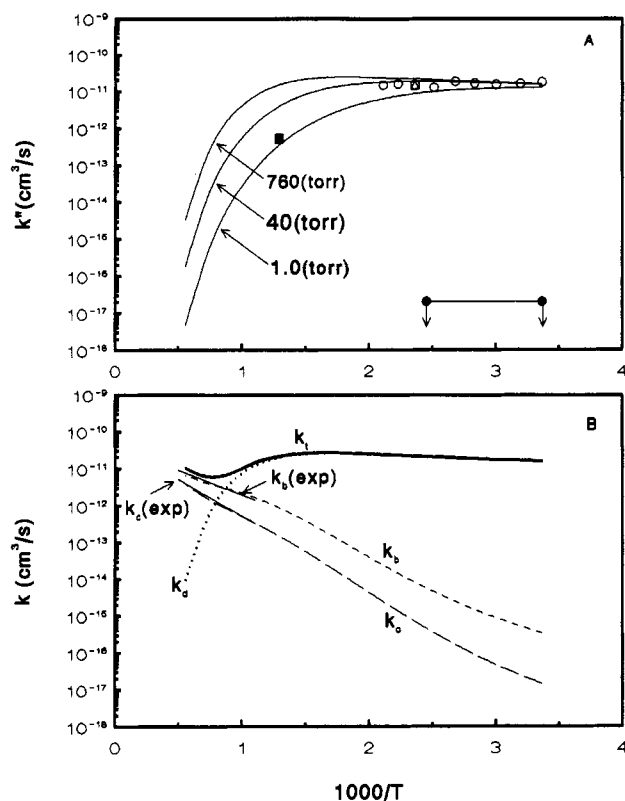


Figure 6. (A) Arrhenius plots of the rate constants for $\text{C}_6\text{H}_5 + \text{O}_2 \rightarrow \text{C}_6\text{H}_5\text{O}_2$ from the experiment (20–80 Torr) and a preliminary RRKM calculation at the indicated pressures: open circles, this work; filled circles, the upper limits set by Preidel and Zellner (ref 17); filled squares, preliminary data of Baldwin et al. obtained at 500 Torr pressure (ref 33). (B) Arrhenius plots of experimental rate constants from ref 30 and the RRKM calculation for the processes of $\text{C}_6\text{H}_5 + \text{O}_2 \rightarrow \text{C}_6\text{H}_5\text{O} + \text{O}$ (k_b), $\text{C}_6\text{H}_5 + \text{O}_2 \rightarrow \text{C}_6\text{H}_4\text{O}_2 + \text{H}$ (k_c), and $\text{C}_6\text{H}_5 + \text{O}_2 \rightarrow \text{C}_6\text{H}_5\text{O}_2$ (k_d) at 2 bar pressure: $k_1 = k_b + k_c + k_d$. The parameters used in the RRKM calculation are presented in Table 3. The step size used in the calculation with Troe's weak-collision approximation is $-\langle\Delta E\rangle = 1$ kcal/mol.

above using the absolute rate constant for the $\text{C}_6\text{H}_5 + \text{c-C}_6\text{H}_{12}$ reaction at 333 K measured by us with the CRD method,¹⁶ $k_{\text{C}_6\text{H}_{12}} = 2.6 \times 10^{-14} \text{ cm}^3/\text{molecule}\cdot\text{s}$, gives rise to $k_{\text{O}_2} = (1.66\text{--}3.6) \times 10^{-11} \text{ cm}^3/\text{molecule}\cdot\text{s}$. Both estimates agree reasonably well with our present value determined at 333 K, $(1.4 \pm 0.1) \times 10^{-11} \text{ cm}^3/\text{molecule}\cdot\text{s}$, considering the uncertainty and errors involved in the above estimate.

More recently, Sommeling et al.²⁰ investigated the reaction of O_2 with the 4-carboxyphenyl radical at 298 K in water using phenol as a probe molecule. They reported $k_{\text{O}_2} = 6.3 \times 10^{-12} \text{ cm}^3/\text{molecule}\cdot\text{s}$, which lies within the range of values estimated above. The result also agrees closely with that obtained by Mertens and von Sonntag,²⁷ $k_{\text{O}_2} = 7.6 \times 10^{-12} \text{ cm}^3/\text{molecule}\cdot\text{s}$, for the phenyl reaction in an aqueous solution at room temperature.

Conclusions

We have measured the rate constant for the appearance of the $\text{C}_6\text{H}_5\text{O}_2$ radical from the $\text{C}_6\text{H}_5 + \text{O}_2$ reaction in the gas phase in the temperature range 297–473 K using the cavity-ring-down method. The reaction was found to be pressure-independent within the range of 20–80 Torr, in agreement with the result of our RRKM calculation. The second-order rate constant for the addition process $\text{C}_6\text{H}_5 + \text{O}_2 \rightarrow \text{C}_6\text{H}_5\text{O}_2$, $k_{\text{O}_2} = 10^{-11.0 \pm 161/T} \text{ cm}^3/\text{molecule}\cdot\text{s}$, is consistent with the values estimated by earlier relative rate measurements in solution, $(0.3\text{--}3.6) \times 10^{-11} \text{ cm}^3/\text{molecule}\cdot\text{s}$ within our temperature range.

A direct probing of the $\text{C}_6\text{H}_5\text{O}$ radical at 473 K by the CRD method at 575 nm, where the radical is known to have a strong absorption band, indicates that it is not formed under the

conditions employed in the present study. This finding is consistent with the result of our RRKM calculation based on the kinetic data of Frank et al. that the formation of the $\text{C}_6\text{H}_5\text{O}$ radical has an apparently large activation energy of 6 kcal/mol. The origin of this large activation energy and the validity of the second product channel producing $\text{H} + o/p\text{-C}_6\text{H}_4\text{O}_2$ (*o*- and *p*-benzoquinones), presumably occurring by a ring-type intermediate such as

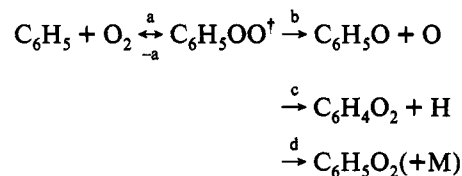


are under investigation. In a companion article, we report an extensive set of structural and energetic data for the stable isomers of $\text{C}_6\text{H}_5\text{O}_2$ obtained by ab initio molecular orbital calculations, which fail to identify the above ring-intermediates as being energetically stable with both ortho and para structures.

Acknowledgment. The authors gratefully acknowledge the support of this work by the Division of Chemical Sciences, Office of Energy Sciences, DOE, under contract No. DE-FG05-91ER14192. Helpful discussions with Professor Robert Louw of Leiden University, the Netherlands, on the $\text{C}_6\text{H}_5 + \text{O}_2$ kinetics and Dr. A. M. Mebel on the structures and energetics of the $\text{C}_6\text{H}_5\text{--O}_2$ system are greatly appreciated. We also thank Prof. C. von Sonntag (Max Planck-Institut für Strahlenchemie, Mülheim, Germany) for communicating with us his unpublished work on the absorption spectra of the phenyl and vinyl peroxy radicals in the visible region.

Appendix: A Preliminary RRKM Calculation for the $\text{C}_6\text{H}_5 + \text{O}_2$ Reaction

We have performed a preliminary RRKM calculation for the $\text{C}_6\text{H}_5 + \text{O}_2$ reaction to illustrate the effect of pressure and temperature under the conditions employed in the present study using a multichannel computer program previously written for the $\text{CH}_3 + \text{O}_2$ reaction.²¹ Although the exact mechanism and the transition states for the association step (a) and the decomposition steps (b) and (c) are not yet well-established, the result of the calculation is helpful to our appreciation of the measured rate constants associated with the three global processes leading to the formation of the adduct and the production of O and H atoms:



At low temperatures ($T < 1000$ K), the addition–stabilization process producing $\text{C}_6\text{H}_5\text{O}_2$ dominates the reaction, whereas under high temperature combustion conditions, the production of the $\text{C}_6\text{H}_5\text{O}$ radical becomes competitive with the stabilization process as illustrated in Figure 6B.

The energetics and molecular parameters of various active species involved in the above mechanism, including the transition states, are summarized in Table 3. As mentioned in the text, the properties of the transition states were estimated by fitting the measured apparent rate constant from this study and those from the work of Frank et al.³⁰ The result of the calculation summarized in Figure 6A,B indicates that the global feature of T/P effects on the three product channels can be well described by the model. It should also be mentioned that RRKM results are usually insensitive to the grouping of vibrational frequencies and the estimate of moments of inertia, as long as the entropy changes (ΔS_i^\ddagger) or the calculated *A* factors for individual channels approximate their experimental values (see, for example, Wieders, G. M.; Marcus, R. A. *J. Chem. Phys.* **1962**, *37*, 1835).